Hierarchical Porous Silica Films with Ultralow Refractive Index

Paolo Falcaro,[†,○] Luca Malfatti,[‡] Tongjit Kidchob,[‡] Giacomo Giannini,[†] Andrea Falqui,[§,||] Maria F. Casula,[||] Heinz Amenitsch,[||] Benedetta Marmiroli,[⊥] Gianluca Grenci,[#] and Plinio Innocenzi*[,‡]

Associazione CIVEN - Nano Fabrication Facility, Via delle Industrie 9, 30175 Marghera, Venezia, Italy, Laboratorio di Scienza dei Materiali e Nanotecnologie (LMNT) and CR-INSTM, D.A.P., Università di Sassari, Palazzo Pou Salid, Piazza Duomo 6, 07041 Alghero, Sassari, Italy, Istituto Italiano di Tecnologia, IIT, Via Morego 30, 16163 Genova, Italy, Dipartimento di Scienze Chimiche and INSTM, Università di Cagliari, S.S. 554 bivio per Sestu, 09042 Monserrato, Cagliari, Italy, Institute of Biophysics and Nanosystems Structure Research, Austrian Academy of Sciences, Schmiedlstrasse 6, A-8042 Graz, Austria, and TASC, INFM National Laboratory, S.S. 14, Km163.5 in Area Science Park, 34012 Basovizza, Trieste, Italy

Received October 9, 2008. Revised Manuscript Received March 4, 2009

Fabrication of hierarchical porous thin films with controlled pore dimension and shape is a current challenge in materials science. In this work, bimodal hierarchical hybrid organic−inorganic thin films with pores in the meso and macro range have been fabricated. The first order of porosity is obtained through a self-assembly process using organic block copolymers as templates for mesopores; the mesophase in the films is well-ordered and has a tetragonal symmetry. We have introduced fluorinated organic nanoparticles of around 70 nm in the precursor solution to act as template of the second order of porosity. The introduction of the nanoparticles has not affected the organization of the mesophase and after the film deposition the nanoparticles become randomly dispersed within the mesostructured matrix. The organization of the mesophase has been studied in situ by small-angle X-ray scattering using synchrotron light; conventional and high-resolution transmission electron microscopy have been used for direct observation of the porosity morphology. The results indicate that hierarchical porous thin films with a bimodal distribution of the pores are obtained upon postsynthesis calcination at 350 °C. The hierarchical porous thin films have a very low refractive index, 1.14 at 633 nm, lower than the 1.17 value measured for the monomodal mesoporous films. The introduction of templating nanoparticles that are removed upon thermal treatment represents, therefore, a successful strategy to decrease the refractive index in porous films. We have also demonstrated that patterning techniques developed for mesostructured films can be successfully extended to this new typology of hierarchical films. Arrays with bimodal hierarchical pore distribution have been fabricated.

Introduction

The preparation of hierarchical porous materials through bottom-up routes represents a current important goal for materials science.[1] The importance of materials with different ranges of porosities is based on the expectation of a new generation of "smart" materials based on hierarchical systems, where the material is able to play a different function in every different pore scale. For this purpose an important issue is controlling the order and topology of the porosity; an ordered porosity is, in fact, a great advantage for applications where diffusion processes are involved.[2]

Significant progress has been made in the preparation of ordered porous materials through self-assembly using a micelle templating synthesis route, which enables good control of pore order and topology.[3] The rising interest in hierarchical materials has realized multirange porosity showing the possibility to select the pore dimensions from a few nanometers up to micrometers. In all the length scales, the larger pores should be connected through the smaller pores and the shape and the connection with the bigger pores must be controlled,[4] in agreement with the definition of hierarchical porous architecture "as a 3D arrangement of well-defined pores of different sizes, the smaller ones being located in the walls between the larger pores, thereby also establishing the connectivity".[5]

Several examples of hierarchical porous materials have been reported so far, but if we focus the attention on thin films with at least one range of porosity showing an ordered structure, we do not find so many examples.[6,7] In the case

* To whom correspondence should be addressed.
[†] Associazione CIVEN - Nano Fabrication Facility.
[‡] Università di Sassari.
[§] Istituto Italiano di Tecnologia.
[||] Università di Cagliari.
[⊥] Austrian Academy of Sciences.
[#] INFM National Laboratory.
[○] Present address: CSIRO Materials Science & Engineering, Gate 5 Normanby Rd, Clayton VIC 3168, Australia.

(1) See, for example, Jaroniec, M.; Schüth, F. Preface to the Special Issue: Templated Materials. *Chem. Mater.* **2008**, *20*, 599.
(2) Nakanishi, K.; Tanaka, N. *Acc. Chem. Res.* **2007**, *40*, 863.
(3) Soler-Illia, G. J. A.; Innocenzi, P. *Chem.−Eur. J.* **2006**, *12*, 4478.
(4) Kuang, D.; Brezesinski, T.; Smarsly, B. *J. Am. Chem. Soc.* **2004**, *126*, 10534.
(5) (a) Sel, O.; Kuang, D.; Thommes, M.; Smarsly, B. *Langmuir* **2006**, *22*, 2311. (b) Sel, O.; Brandt, A.; Wallacher, D.; Thommes, M.; Smarsly, B. *Langmuir* **2007**, *23*, 4724.
(6) Tao, S.; Yin, J.; Li, G. *J. Mater. Chem.* **2008**, *18*, 4872.
(7) Williford, R. E.; Fryxell, G. E.; Li, X. S.; Addleman, R. S. *Microporous Mesoporous Mater.* **2005**, *84*, 201.

10.1021/cm802750w CCC: $40.75
Published on Web 04/27/2009

of bulk or powdered materials two kind of processes have been reported: the addition of a block copolymer and a small surfactant or cosolvent to the sol−gel solution;[8−10] infiltration of sol−gel solution containing block copolymers in a presynthesized polymeric colloidal crystal structure.[11−13] In general, two main strategies can be envisaged, controlled phase separation or addition of surfactant templates of different dimensions to control the pores. We propose here a different approach to obtain hierarchical porous thin film: the use of predefined nano-objects such as nanoparticles of controlled dimension as template for the pore of bigger dimensions. The main advantage of this strategy is the easy removal of the template without disrupting the host material. We have used a self-assembled mesostructured hybrid organic−inorganic thin film as the matrix of the nanoparticles. This route has allowed us to introduce removable nano-objects into a mesoporous material, which gives after thermal treatment at 350 °C a bimodal porous film with pores in the 9 and 60 nm ranges.

Experimental Section

Preparation of Nanoparticles Colloidal Solution. 2,2,2-Trifluoroethyl methacrylate (TFEMA, TOSO Chemicals) was distilled in vacuum and stored under nitrogen at −20 °C. Potassium persulfate (KPS, Fluka), sodium bicarbonate (Fluka), sodium dihydrogenphosphate (NaH_2PO_4, Aldrich), Brij 58 (polyethoxylated cetyl alcohol with 20 oxyethylene units, Fluka), and sodium dodecylsulfate (SDS, Fluka) were used as-received. HPLC-grade water was used for the polymerizations.

The nanoparticles colloidal solution (NCS) was prepared by seeded semicontinuous emulsion polymerization by adapting a procedure described by Castelvetro et al.[14] The polymerization was carried out under a nitrogen atmosphere in a conventional 250 mL jacketed glass reactor equipped with thermostatted bath circulator, reflux condenser, mechanical stirrer, and thermocouple. The seed latex was prepared directly in situ by a batch process. The reactor containing a solution of SDS (0.6 g) in 90 mL of deionized water was loaded with the monomer (TFEMA, 10 g), purged with nitrogen for 30 min, and then heated at 70 °C under stirring (250 rpm) prior to addition of the initiator (0.15 g of KPS in 5 mL of water). After 2 h of polymerization at 70 °C, two distinct and individually deoxygenated feeds with TFEMA (20 g) and the aqueous solution of surfactant (Brij 58P, 0.15 g), buffer ($NaHCO_3$, 0.035 g; NaH_2PO_4, 0.035 g), and initiator (KPS 0.06 g), respectively, were added by means of metering syringe pumps. During the feeding stage and throughout the polymerization the mixture in the reactor was stirred at 250 rpm and the circulating thermostatted fluid maintained at 70 °C. The feeds were added simultaneously for 3 h, and the polymerization was then allowed to proceed for an additional 2 h. The resulting seed latex, with 19.9 wt % solids, contained monodispersed polymer particles of average diameter $d_p = 69$ nm and polydispersity index, PDI, equal to 0.036 according to photon correlation spectroscopy (PCS) analysis. No additional peak due to surfactant micellization was observed in the intensity distribution.

The number of particles contained in 1 kg of NCS was estimated as $N_p = 8.33 \times 10^{17}$ kg^{-1}. This value is calculated from the measured particle size according to the following expression:

$$N_p = \frac{6 \text{ wt \%}}{\pi \rho d_p^{\,3}} \quad (1)$$

where wt % is the weight fraction of polymer in the NCS (19.9%), ρ is the polymer density (estimated as 1.39 g·cm^{-3}), and d_p is the intensity-average particle diameter as determined by PCS (69 nm). The density of NCS was not determined, but it can be reasonably approximated as 1 g·cm^{-3} so that volume and weight have been used interchangeably.

Hierarchical Mesostructured Films. Triblock copolymer surfactant (Pluronic F127), tetraethylorthosilicate (TEOS), methyltriethoxysilane (MTES), and ethanol (EtOH) were purchased from Aldrich and used as-received.

P-type/boron-doped, (100) oriented, 400 μm thick silicon wafers (Si-Mat) were employed as the substrates. A stock solution was prepared, adding EtOH (31 mL), TEOS (29 mL), MTES (13 mL), and HCl (4 mL, 0.9 M). This sol was left to react under stirring in a closed vial for 45 min at room temperature. Seven different precursor solutions were prepared as a function of nanoparticles concentration adding respectively 0.3, 0.6, 0.9, 1.2, 1.5, 3, and 6 mL of NCS to a mixture of Pluronic F127 (1.3 g), EtOH (15 mL), and HCl aqueous solution (6×10^{-3} M, 1.5 mL). The final precursor solutions were obtained by adding 7.7 mL of stock solution to the templating solutions and reacting the sols under stirring for 1 h at room temperature; the [F127]/[Si] molar ratio in the final sol was $\approx 5 \times 10^{-3}$ M.

To fabricate patterned hierarchical porous films by deep X-ray lithography, the precursor solutions were modified by the addition of 0.3 mg of a photoacid initiator: bis(4-*tert*-butylphenyl)iodonium *p*-toluenesulfonate (Aldrich).

To prepare hierarchical films, silicon substrates, previously cleaned with water and EtOH and rinsed with acetone, were dip-coated in the precursor solutions (withdrawal speed = 2.3 mm·s^{-1}) at relative humidity (RH%) between 20 and 40%. After dip coating, the samples were dried at 60 °C for 1 h and then calcined at 350 °C for 1 h.

Materials Characterization. Polymeric nanoparticle sizes were determined by PCS using a Brookhaven 90 Plus Dynamic Laser light scattering instrument. Particle size, particle size distribution, and polydispersity index were calculated from the autocorrelation function using CONTIN and NNLS data elaboration.

An in situ study of self-assembly process was performed on as-deposited films by 2D grazing incidence small-angle X-ray scattering (GISAXS) at the Austrian SAXS beamline at Elettra with an incident wavelength of 1.54 Å. The incident energy was set at 8 keV. The instrumental glancing angle between the incident radiation and the sample was set slightly above the critical angle, which is in grazing incidence mode. A 2D CCD detector (Photonic Science, UK) was used to acquire the scattering patterns. RH% has been controlled by a pneumatic valve able to combine together dry and wet air, obtaining bubbling dry air in a heated water solution. RH% and temperature were recorded during every experiment by a temperature−humidity data logger (PICO-meter RH02).

Information on the morphology of the samples was obtained by transmission electron microscopy (TEM) using a JEOL 200CX microscope equipped with a tungsten cathode operating at 200 kV.

(8) Nakanishi, K.; Kobayashi, Y.; Amatani, T.; Hirao, K.; Kodaira, T. *Chem. Mater.* **2004**, *16*, 3652.
(9) Jinnai, H.; Nakanishi, K.; Nishikawa, Y.; Yamanaka, J.; Hashimoto, T. *Langmuir* **2001**, *17*, 619.
(10) Smarsly, B.; Polarz, S.; Antonietti, M. *J. Phys. Chem. B* **2001**, *105*, 10473.
(11) Li, F.; Wang, Z.; Ergang, N. S.; Fyfe, C. A.; Stein, A. *Langmuir* **2007**, *23*, 3996.
(12) Antonietti, M.; Berton, B.; Goltner, C.; Hentze, H. P. *Adv. Mater.* **1998**, *10*, 154.
(13) Kuang, D. B.; Brezesinski, T.; Smarsly, B. *J. Am. Chem. Soc.* **2004**, *126*, 10534.
(14) Castelvetro, V.; De Vita, C.; Giannini, G.; Simone, G. *J. Appl. Polym. Sci.* **2006**, *102*, 3083.

Finely ground films scratched from the silicon substrate were dispersed in *n*-octane by sonication, and then they were dropped on a carbon-coated copper grid and dried for TEM observations. High-resolution transmission electron microscope (HRTEM) images were obtained by a JEOL 2100F transmission electron microscope equipped with a field emission electron gun and operating at 200 kV. The samples were prepared for cross-section or planar view analysis: two small plates were prepared by cutting the sample at a fixed height of the substrate. A roughly mechanical polishing procedure was carried out on all the samples to achieve around 50 μm in thickness: in the direction parallel to the substrate cut for the cross-section sample and in the direction perpendicular to the substrate cut for the planar view sample. Final thinning to electron transparency was achieved by precision ion milling with a JEOL IS (Ion Slicer).

Refractive index and thickness were measured by a α-SE Wollam spectroscopic ellipsometer. The measurements were done at room temperature; *n*, *k*, and the residual porosity were calculated by 2.03 α-SE Wollam software.

Fourier transform infrared (FTIR) analysis was performed using a Nicolet Nexus spectrophotometer. The spectra were recorded in transmission, in the 400−5000 cm^{-1} range, by averaging 256 scans with 4 cm^{-1} resolution; a silicon wafer was used as substrate to measure the background.

Film Lithography. The as-deposited films were patterned 3 h after the deposition at the Deep X-ray Lithography (DXRL) beamline of Elettra synchrotron facility (Trieste, Italy). The samples were exposed through X-ray masks containing test patterns of different sizes (from 20 to 500 μm), shape, and geometry. The masks had a 20 mm thick gold absorber and a transparent membrane of titanium with a thickness of 2.2 mm. The deposition dose on the bottom of the film was 3 $kJ \cdot cm^{-3}$. After 12 h since exposure to X-rays, the films were chemically etched to remove the nonirradiated parts of the sample. The developing solution was prepared by mixing ethylene glycol (35 mL) and ethanol (10 mL); the samples were sonicated for 20−30 s in the solution, and then they were dried under an air flow. The solution was optimized to obtain the etching in a time scale of seconds and the maximum aspect ratio for the patterned structures. The films, after the lithographic process, were thermally treated at 350 °C for 1 h.

Results and Discussion

Porous Structure. The fabrication of mesoporous hierarchical films with controlled porosity is the main task of the work. We have used evaporation-induced self-assembly (EISA) to obtain highly organized mesostructured films templated by block copolymers with an ordered mesophase in the 8−10 nm range and polymeric nanospheres to produce pores of around 50−60 nm within the mesostructured films. The introduction of the nanospheres, especially at high concentrations, could potentially interfere with self-assembly. We have, therefore, used in situ SAXS analysis to study the mesophase formation in hybrid organic−inorganic films synthesized via EISA[15] and the effect of nanospheres on self-organization. The SAXS technique gives fundamental information to identify the mesophase[16] and investigate the kinetics of mesostructure formation.[17] Time-resolved SAXS images showing mesostructure formation have been collected by employing GISAXS. Figure 1a shows a typical GISAXS pattern of a sample prepared with 3 mL of NCS and treated at 350 °C. The presence of well-defined spots is a clear indication of an ordered mesostructure within the hybrid film. The pattern can be assigned to a tetragonal symmetry (space group *I*4/*mmm*) with the (100) plane oriented perpendicular to the substrate (Figure 1b), in accordance with previous findings.[18] This organization corresponds to an ordered stack of spherical pores with a body-centered tetragonal primitive cell. Comparing these results with those of hybrid MTES−TEOS mesoporous films,[19] we can observe that the presence of NCS, even at high concentrations, does not affect the self-assembly: no appreciable variations in terms of degree of order or mesophase symmetry are detectable by changing the relative amount of NCS in hierarchical films.

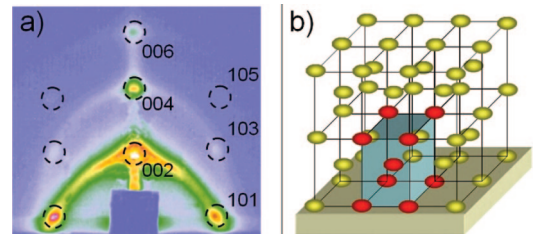

Figure 1. (a) GISAXS pattern of a hierarchical mesoporous hybrid film treated at 350 °C (3 mL of NCS in the precursor sol). (b) Body-centered tetragonal (*I*4/*mmm* in the space group) porous structure image.

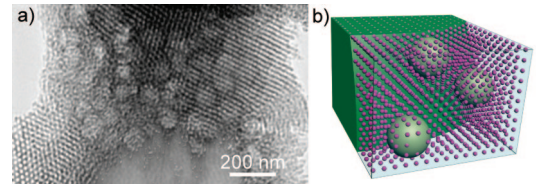

Figure 2. Dark-field TEM image of a hierarchical porous thin film treated at 350 °C (a) and a representative picture of the hierarchical structure (b).

We have obtained a direct visualization of the film porous structure using transmission electron microscopy in conventional and high-resolution mode. Figure 2a shows the TEM image of a scratched fragment of the porous film after thermal treatment at 350 °C. The mesophase organization is well-preserved, even after calcination, and the nanoparticles are dispersed within the matrix. The hierarchical structure that appears from this image is shown in Figure 2b and is made from an ordered distribution of mesopores and a random distribution of pores of larger dimensions (around 60 nm) produced by the thermal removal of the polymeric nanoparticles.

Figure 3a,b shows a HRTEM cross-section image of the film after curing for 2 h at 350 °C; a planar section of the

(15) Grosso, D.; Babonneau, F.; Sanchez, C.; Soler-Illia, G. J. A. A.; Crepaldi, E. L.; Albouy, P. A.; Amenitsch, H.; Balkenende, A. R.; Brunet-Bruneau, A. *J. Sol-Gel Sci. Technol.* **2003**, *26*, 561.
(16) Tate, M. P.; Hillhouse, H. W. *J. Phys. Chem. C* **2007**, *111*, 7645.
(17) Innocenzi, P.; Malfatti, L.; Kidchob, T.; Falcaro, P.; Costacurta, S.; Piccinini, M.; Marcelli, A.; Morini, P.; Sali, D.; Amenitsch, H. *J. Phys. Chem. C* **2007**, *111*, 5345.
(18) Falcaro, P.; Costacurta, S.; Mattei, G.; Amenitsch, H.; Marcelli, A.; Cestelli Guidi, M.; Piccinini, M.; Nucara, A.; Malfatti, L.; Kidchob, T.; Innocenzi, P. *J. Am. Chem. Soc.* **2005**, *127*, 3838.
(19) Innocenzi, P.; Malfatti, L.; Kidchob, T.; Falcaro, P.; Cestelli Guidi, M.; Piccinini, M.; Marcelli, A. *Chem. Commun.* **2005**, 2384.

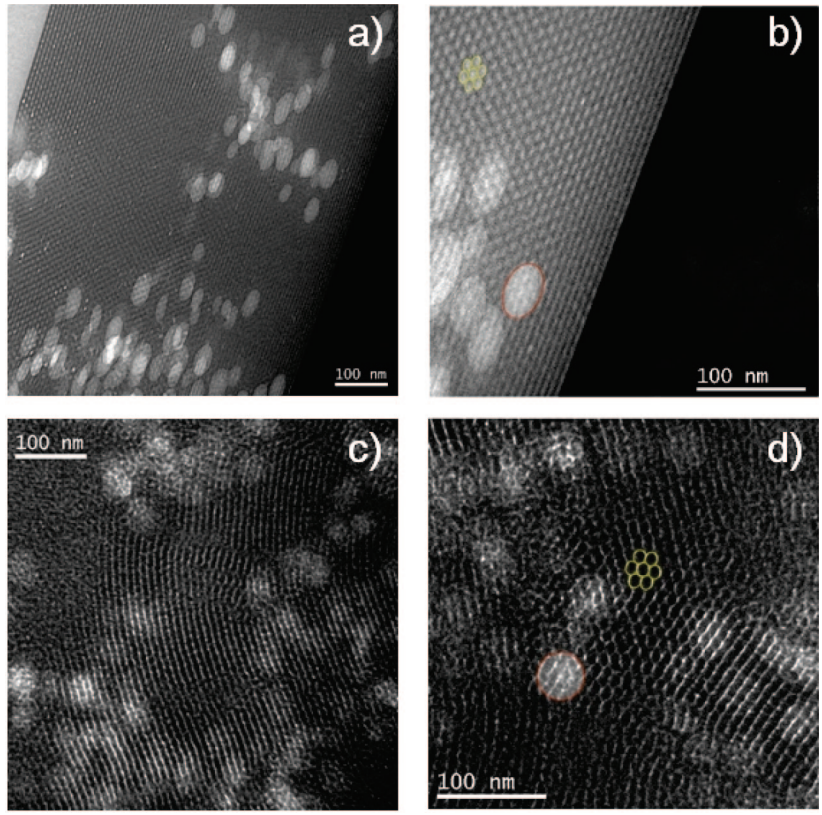

Figure 3. Dark-field cross-section (a and b) and planar view (c and d) HRTEM images of a hierarchical porous thin film treated at 350 °C. The macropores produced by the polysterene nanospheres appear as white spots in the images.

same sample is shown in Figure 3c,d. A bimodal pore distribution is clearly detected from both cross and planar sections; the film is characterized by an ordered lattice of 9 nm pores and a random distribution of 60 nm pores. The HRTEM figures show an apparent coalescence of close pores, which is however due to the artifact of TEM images that merges a tridimensional structure in a plane. The different gray scale of the larger pores indicate that they are spatially separated. The mesostructure is highly ordered within a range of some micrometers; the cross section shows that the film maintains a well-ordered porous structure along all the directions normal to the substrate (Figure 3a). The planar view shows that the mesostructure has grain domains of organized pores at micrometer scale (Figure 3c). No effects induced by polymer nanoparticles on the ordered mesophase have been observed: in the range of composition investigated, NCS and the surfactant work separately. The pore dimensions have been calculated from the cross-section HRTEM images: along the direction parallel to the substrate, the average size of pores templated by the nanoparticles is 55 ± 10.4 nm; along the direction perpendicular to the substrate, the average size is 26 ± 3.7 nm. We have also calculated the dimensions of mesopores: in this case the average size in the directions perpendicular and parallel to the substrate are 8.8 ± 0.9 and 4.8 ± 1.2 nm, respectively. Comparing the cross section (Figure 3b) to the planar section (Figure 3d), we observe that the thermal calcination induces a shrinkage in the direction normal to the substrate; this affects the pore shape of both the smaller and bigger pores, producing an ellipsoidal shape. The average ratio between the shorter axis (perpendicular to the substrate) and the longer axis (parallel to the substrate) of the different ranges of pores has been calculated by HRTEM; we obtained a value of 0.47 for the larger pores and 0.54 for the smaller pores. This indicates that the thermal shrinkage of the films induces similar eccentricity on both the pore distributions. If we look at the pores in the planar section image, we can observe that they have a regular and circular shape (Figure 3d), whereas an elliptical shape emerges from the HRTEM cross-section image (Figure 3b). In the present case the thermal shrinkage produces a deformation of the pore shape with a contraction in the direction normal to the substrate without, however, a change in the mesophase,[20] which maintains a tetragonal symmetry after calcination, in both the mesoporous and the hierarchical films.

Properties. The SAXS and TEM analysis show that our "one-pot" single-step synthesis produces a bimodal pore distribution with 9 nm ordered pores of tetragonal symmetry and 60 nm randomly dispersed pores in the film. The fabrication of this bimodal hierarchical porous film is achieved by removal of the templates, i.e., the micelles for mesopores and the nanoparticles for the macropores, by thermal treatment. We have, therefore, observed by FTIR analysis and spectroscopic ellipsometry the effect of the thermal calcination on composition and properties of the films. We have compared the FTIR and ellipsometry data of as-deposited and 350 °C calcined samples to assess the removal of the templates. Parts (a) and (b) of Figure 4 show the FTIR spectra of mesoporous and hierarchical films,

(20) Innocenzi, P.; Malfatti, L.; Kidchob, T.; Falcaro, P.; Costacurta, S.; Guglielmi, M.; Mattei, G.; Amenitsch, H. *J. Synchr. Radiat.* **2005**, *12*, 734.

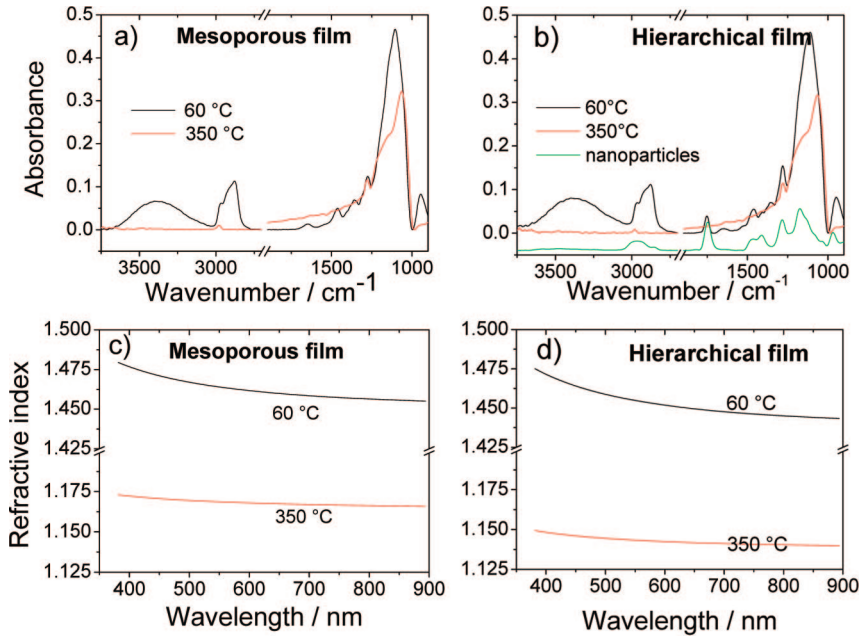

Figure 4. FTIR absorption spectra of mesoporous hybrid film (a) and a hierarchical porous film (b) after thermal treatment at 60 °C (black line) and 350 °C (red line). The reference spectrum of nanoparticles is shown in (b). The refractive index as a function of the wavelength for a mesoporous film (c) and a hierarchical porous film (d) after thermal treatment at 60 °C (black line) and 350 °C (red line).

respectively, before (60 °C) and after thermal treatment (350 °C). We take the signal around 1700 cm^{-1}, which is assigned to carbonyl groups (C═O stretching), as a signature of the presence of the polymeric nanoparticles (Figure 4b);[21] the FTIR spectrum of the nanoparticles alone is reported as a reference (green line). The thermal treatment removes the nanoparticles, the signal at 1700 cm^{-1} disappears, and the surfactant (the CH_2 stretching bands around 2700 cm^{-1}, which indicate the presence of the block copolymers, also disappear after calcination).[21] Another effect of the thermal treatment is the removal of silanols; the wide OH stretching band around 3300 cm^{-1} disappears.[22] Noteworthy, the methyl groups are still present in the films after calcination at 350 °C, and this is correlated with the absence of adsorbed molecular water. The change in refractive index between the samples treated at 60 and 350 °C (Figure 4c,d) reflects the thermal shrinkage and the removal of the organic components; after calcination, the hierarchical porous films have a lower refractive index that we attribute to a lower porosity. The refractive index values measured at 633 nm are 1.14 and 1.17 for the hierarchical mesoporous and monomodal mesoporous films, respectively. The thickness of the films changes from 815 to 628 nm in the mesoporous films and from 1185 to 975 nm in the hierarchical films (6 mL of NCS in the precursor sol). The data have been obtained assuming a fitting model based on the assumption of transparent films (the measurements have been done in the 390−900 nm range—in this interval the doped film does not absorb) on silicon (Cauchy dispersion relation).[23] The quality of the fitting was evaluated on the ground of the mean square error. A Bruggeman effective medium approximation[24] layer with two components (nonabsorbing Cauchy film and void) has been used to evaluate the refractive index. The residual porosity after the thermal calcination is still high, around 60% in volume for the mesoporous films and 69% in volume for the hierarchical samples (6 mL of NCS in the precursor sol). The amount of nanoparticles affects the films properties; higher contents of nanoparticles increase the thickness and the residual porosity. Figure 5 shows the film thickness as a function of NCS volume introduced in the precursor solution for films treated at 60 and 350 °C; the values have been calculated by the ellipsometric data. In the inset of Figure 5 is shown the dependence of the porosity on the amount of nanoparticles for the films calcined at 350 °C.

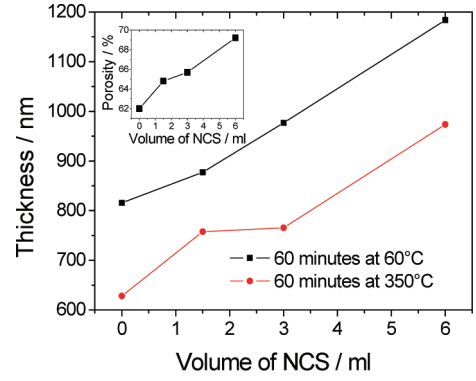

Figure 5. Variation of film thickness as a function of nanoparticles content in the precursor solution (in milliliters of NCS) after thermal treatment at 60 °C (black line) and 350 °C (red line). In the inset is shown the dependence of the porosity on the nanoparticles content for hierarchical porous films treated at 350 °C.

(21) Colthup, N. B.; Daly, L. H.; Wiberley, S. E. *Introduction to Infrared and Raman Spectroscopy*; Academic Press: San Diego, 1990.
(22) Innocenzi, P. *J. Non-Cryst. Solids* **2003**, *316*, 309.
(23) The Cauchy dispersion equation, $n(\lambda) = A_n + B_n/\lambda^2 + C_n/\lambda^4$, allows calculating the refractive index as a function of the wavelength. A_n is a parameter related to the average refractive index of the material, whereas B_n and C_n are parameters that provide the shape or curvature of the $n(\lambda)$ curve.
(24) For a two-components material, the refractive index in the Bruggemann approximation is expressed as $f_v[(n_v^2 - n^2)/(n_v^2 + 2n^2)] + f_{SiO_2}[(n_{SiO_2}^2 - n^2)/(n_{SiO_2}^2 + 2n^2)] = 0$ where f_v, n_v and f_{SiO_2}, n_{SiO_2} are the volume fractions and the refractive index of the pores void and silica, respectively.

The properties of these mesoporous and hierarchical porous films after calcination appear particularly interesting; the presence of residual methyl groups upon calcination at 350 °C inhibits the adsorption of water from the external environment and they exhibit an ultralow refractive index, among the lowest values for those reported in the literature for silica-based porous materials.[25−27] For comparison a value of $n = 1.18$ in the 350−800 nm visible range and $n = 1.14$ at $\lambda = 1300$ nm has been reported for hierachical porous silica films,[28] $n = 1.21-1.23$ for silica mesoporous films prepared using an ionic surfactant[27] and 1.17 at $\lambda = 500$ nm in the case of MTES−TEOS mesoporous films.[29] These results show that a lower refractive index and a higher residual porosity can be obtained in hierarchical porous films, which have applications as ultralow k[30] and ultralow refractive index materials.[31,32]

Top-Down Film Patterning Technology. An important condition to develop applications based on mesoporous thin films is that patterning technologies, such as lithographic techniques, are available.[33] We have, therefore, applied to hierarchical mesostructured films an X-ray lithography technique, previously developed for silica mesoporous films, to produce patterned layers.[34] The precursor solutions have been modified by adding a photoacid initiator and films have been deposited following the same deposition procedure that was applied to obtain mesoporous and hierarchical films. SAXS measurements in situ have been used to detect the mesostructure formation and any change in the organization that could be induced by the addition of the photoacid generator in the precursor solution. The same self-assembly process has been observed: the photoacid initiator in the precursor sol does not affect the mesostructure formation. The samples have then been exposed to X-ray radiation using a synchrotron source; the exposure of the films to X-rays has not caused any structural change in the mesophase[35] or damage such as cracking. The lithographic method allows transferring the mask pattern to the material (Figure 6); this patterning method is based on the simultaneous selective template removal and silica polycondensation induced by synchrotron radiation in the exposed region.[31] During the etching process the unexposed region is easily removed from the substrate, leaving a patterned area. An important advantage of this method is the possibility to remove the template and to induce condensation of the silica network in a single-step process.[31]

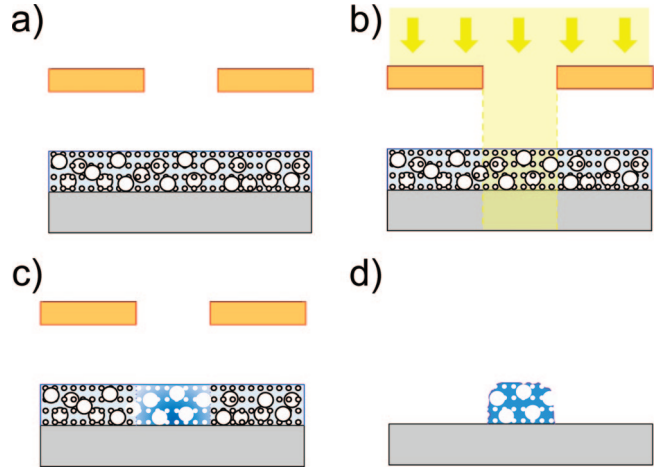

Figure 6. Sketch of the lithographic process by deep X-ray lithography: (a) a hierarchical film is produced and exposed after deposition of X-ray through a mask (b), the X-rays induce a condensation of the silica network and removal of the surfactant to the exposed side (c), and the final etching process removes the unexposed part of the film and produces a patterned hierarchical structure (d).

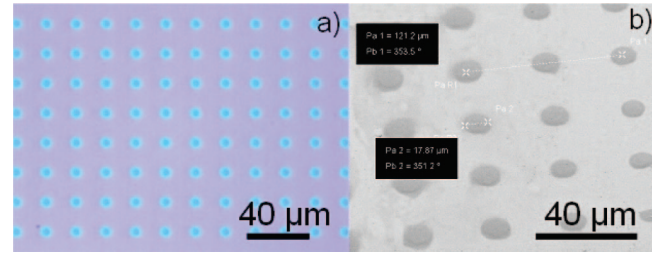

Figure 7. Optical microscopy image of patterned hierarchical porous films before etching. (a) The patterned objects can be discerned by their color because of the difference in refractive index between the masked (dark blue) and the unmasked regions (light blue). (b) SEM image of the same film after chemical etching; an array of dots of ca. 20 μm is formed.

Figure 7a shows an optical image of an array with dots of ca. 20 μm diameter. The film has been treated at 60 °C and the film thickness is around 200 nm; the film is not etched and the difference in color is due to the change of refractive index between the exposed (light blue) and unexposed side of the sample (blue). Regular pillars have been obtained at the end of the process; after etching, the SEM image shows the formation of a highly regular array of dots (Figure 7b).

Conclusions

Hierarchical mesoporous thin films have been obtained by using block-copolymer micelles and organic polymer nanoparticles of 70 nm as templates of pores of different dimensions. Evaporation-induced self-assembly is used to prepare a mesoporous matrix for the nanoparticles that are entrapped and well-dispersed within the film. The introduction of the nanoparticles into the precursor solution does not affect the self-assembly process; a tetragonal mesostructure with *I*4/*mmm* symmetry is obtained in the films. A thermal treatment at 350 °C removes the organic template and the

(25) Falcaro, P.; Grosso, D.; Amenitsch, H.; Innocenzi, P. *J. Phys. Chem. B* **2004**, *108*, 10942.
(26) Maruo, T.; Tanaka, S.; Hillhouse, H. W.; Nishiyama, N.; Egashira, Y.; Ueyama, K. *Thin Solid Films* **2008**, *516*, 4771.
(27) Pénard, A.-L.; Gacoin, T.; Boilot, J.-P. *Acc. Chem. Res.* **2007**, *40*, 895.
(28) (a) Konjhodzic, D.; Bretinger, H.; Wilczok, U.; Dreier, A.; Ladenburger, A.; Schmidt, M.; Eich, M.; Marlow, F. *Appl. Phys. A: Mater. Sci. Process.* **2005**, *81*, 425. (b) Konjhodzic, D.; Schroeter, S.; Marlow, F. *Phys. Status Solidi A* **2008**, *204*, 3676.
(29) (a) De Theije, F. K.; Balkenende, A. R.; Verheijen, M. A.; Baklanov, M. R.; Mogilnikov, K. P.; Furukawa, Y *J. Phys. Chem. B* **2003**, *107*, 4280. (b) Balkenende, A. R.; De Theije, F. K.; Kriege, J. C. K. *Adv. Mater.* **2003**, *15*, 139.
(30) Hatton, B. D.; Landskron, K.; Hunks, W. J.; Bennett, M. R.; Shukaris, D.; Perovic, D. D.; Ozin, G. A. *Mater. Today* **2006**, *9*, 22.
(31) Maruo, T.; Tanaka, S.; Nishiyama, N.; Motosa, K. I.; Funayama, K.; Egashira, Y.; Ueyama, K. *Colloids Surf. A* **2008**, *318*, 84.
(32) Grosso, D.; Boissiere, C.; Sanchez, C. *Nat. Mater.* **2007**, *6*, 572.
(33) Innocenzi, P.; Kidchob, T.; Falcaro, P.; Takahashi, M. *Chem. Mater.* **2008**, *20*, 607.
(34) Falcaro, P.; Costacurta, S.; Malfatti, L.; Kidchob, T.; Takahashi, M.; Casula, M.; Piccinini, M.; Marcelli, A.; Marmiroli, B.; Amenitsch, H.; Schiavuta, P.; Innocenzi, P. *Adv. Mater.* **2008**, *20*, 1864.
(35) Malfatti, L.; Kidchob, T.; Costacurta, S.; Falcaro, P.; Schiavuta, P.; Amenitsch, H.; Innocenzi, P. *Chem. Mater.* **2006**, *18*, 4553.

nanoparticles without producing cracking in the films and leaving a bimodal porous hierarchical structure. Two ranges of well-defined porosities are produced: (1) mesoporosity due to the organic templating micelles with an average pore dimension of 9 nm (these pores are also well-ordered following a tetragonal unit cell); a porosity in the 60 nm range, which is produced by the thermal removal of the polymeric nanoparticles (these pores are not ordered but are well-dispersed within the mesoporous matrix).

The process that we have developed allows obtaining hierarchical porous films with an ultralow refractive index combined with hydrophobicity. The process is compatible with X-ray lithographic techniques; microdot arrays with bimodal porous distribution have been fabricated.

Acknowledgment. This research was supported by the Italian Ministero dell'Università e della Ricerca (MiUR) through FIRB2003 (RBNE033KMA). Dr. Luca Businaro is gratefully acknowledged for helpful support at the DXRL beamline in Elettra.

CM802750W